3D-Printed Calorimetric Flow Sensor

Gerjan Wolterink[1,2], Ameya Umrani[1], Martijn Schouten[1], Remco Sanders[1], Gijs Krijnen[1]
[1]Robotics And Mechatronics group, [2]Biomedical Signal and Systems
University of Twente, Enschede, The Netherlands, Email: gerjan.wolterink@utwente.nl

***Abstract* - This work shows the development and characterization of a fully 3D-printed thermal mass flow sensor, based on regular and carbon-doped thermoplastic polyurethane (TPU). Using multi material fused deposition modelling (FDM) 3D-printing, the sensor is based on one heater element and two resistive thermal sensors (sensor - heater - sensor configuration). The transduction is based on the temperature dependent resistance of carbon doped polymers. Characterisation of the conductive TPU shows a positive thermal coefficient of resistance (TCR) ranging between 0.002 °C^{-1} to 0.024 °C^{-1}, whereas the sensor shows a responsivity of 20 mV ml^{-1} min^{-1} in the pseudo linear range for flows below 3 mL min^{-1} while using a power of 1 W and a temperature up 58 °C.**

Keywords - 3D-Printing, Calorimetric, Flow Sensing, FDM, Conductive TPU

I. Introduction

3D-printed sensors are of interest for small volume, distributed fabrication, customisation and integration in 3D-printed structures. These advantages also count for microfluidic structures due to a small number of required fabrication steps to create 3D geometries and customisation at low cost. 3D-printing also allows for the creation of functional sensing structures that can be embedded in microfluidic structures [1], [2]. A 3D-printed Venturi tube for flow sensing has been demonstrated by Ademski et al. [1], Leigh et al. [3] have demonstrated an impeller flow sensor made using used fused deposition modeling (FDM) technology. However both methods are hybrid approaches and additional commercial sensors needed to be placed inside the structure. Recently a 3D printed flow sensor, with additional metallization, based on the Coriolis effect was presented [4].

In this work we show a proof of concept calorimetric flow sensor, completely fabricated using a consumer grade multi-material FDM 3D-printer, without the need for additional sensors since the conductive material functions as heater and sensor. Previously reported 3D printed sensors printed in one go using FDM technology are mainly resistive and capacitive force sensors and do not use the thermal properties of the conductive material [5]–[10].

II. Sensor principle

A. Calorimetric Flow Sensing

In calorimetric flow sensing, heat is injected in a flow and the corresponding temperature change due to convection is measured at a certain distance. One implementation uses two thermal sensors and a heater. Relative to the flow-direction, one sensor is placed upstream, whereas the second one is located downstream [11], [12]. The heated fluid is transported from the heater by the flow resulting in a thermal gradient, causing the upstream temperature to fall and the downstream temperature to rise. The heating is provided by joule heating, resulting in a temperature increase in the fluid. The resistance of the thermal sensors change according to temperature and in a certain flow range the difference in temperature is resolved as a resistance difference proportional to the heat transported by the flow. As such, it is a direct measurement of the heat flow, and an indirect measurement of fluid velocity [11]. The principle of the calorimetric flow sensing is illustrated in Figure 1.

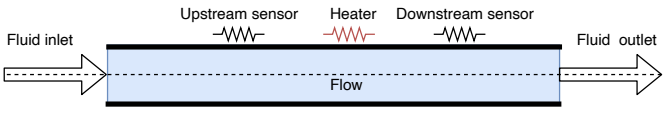

Fig. 1. Schematic representation of a calorimetric flow sensor.

B. Model

In our sensor geometry the flow is unidirectional through a circular duct formed in a 3D printed structure which consists of two concentric sensors and one concentric heater, see Figure 2 left. We consider a one-dimensional heat transfer model with flow velocity and temperature averaged over the cross-section.

$$\rho c_{\mathrm{p}}\left[\frac{\partial T}{\partial t}+v\frac{\partial T}{\partial x}\right]-k\frac{\partial^2 T}{\partial x^2}=\frac{Q(x)}{A} \tag{1}$$

Where c_{p} is the specific heat, ρ the fluid density, k the thermal conductivity of the fluid, v the average velocity of the flow in x-direction, A the cross-section of the tube and Q the heat density, which is only non-zero at the position of the heater. Introducing boundary conditions at the edges of the heater and assuming the temperature at the ends of the sensor structure to be at ambient temperature, for time independent flow the solution to the simplified system reads:

$$T(x,v)=\begin{cases}A_1 e^{\rho c_{\mathrm{p}} x/k}+B_1, & -L\le x\le -x_{\mathrm{h}}\\ \frac{1}{\rho c_{\mathrm{p}} v}\left[A_{\mathrm{c}} k e^{\rho c_p x/k}+Qx\right]+B_{\mathrm{c}}, & |x|\le x_{\mathrm{h}}\\ A_2 e^{\rho c_{\mathrm{p}} x/k}+B_2, & x_h\le x\le L\end{cases} \tag{2}$$

where $2L$ is the length of the sensor, x_{h} is half the heater length and A_i and B_i, $i=1,2,\mathrm{c}$ implicitly depend on v.

978-1-7281-6801-2/20/$31.00 ©2020 IEEE

Figure 2 shows the effect of the v on the temperature inside the tube for deionized water. v ranges from $0\,\mathrm{mm\,s^{-1}}$ to $100\,\mathrm{mm\,s^{-1}}$ assuming a constant power of $300\,\mathrm{mW}$ supplied to the heater.

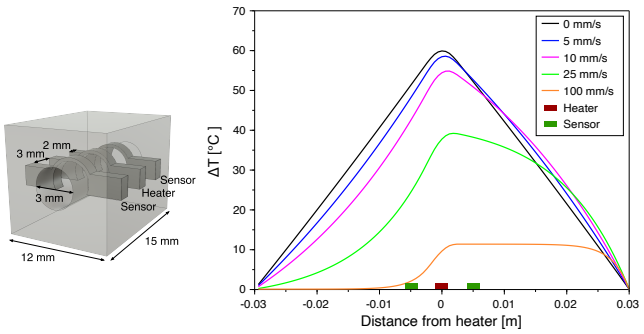

Fig. 2. Left: CAD file of the sensor. Right: temperature profile for various flow velocities.

III. Methodology

A. Sensor design and Fabrication

Figure 2 left shows the CAD file of the flow sensor with a total length of $15\,\mathrm{mm}$, the diameter of the circular channel is $3\,\mathrm{mm}$. The heater is located at the centre of the channel and has a width of $2\,\mathrm{mm}$ the two sensors also have a width of $2\,\mathrm{mm}$ and are placed symmetrically at a $3\,\mathrm{mm}$ distance from the heater. The location of the sensing resistors is chosen based on the analytical expression eq. 2. The rectangular outside allowed for easy printing without the need for support material. The flow sensor is printed using a dual nozzle FDM 3D-printer (Creator Pro, FlashForge Corporation, China) fitted with a dedicated extrusion system for flexible materials (Flexion Extruder, Diabase Engineering, USA). The sensors and heaters are made of conductive TPU (PI-ETPU 85-700+, Palmiga Innovation, Sweden), the rest of the flow sensor structure is printed from non-conductive TPU (NinjaFlex SemiFlex, Fenner Drives, USA).

B. Thermal characterisation of conductive TPU

To determine the thermal properties of the conductive TPU material a $10\,\mathrm{cm}$ sample with a diameter $1.75\,\mathrm{mm}$ was placed in a computer controlled oven. The temperature was increased from $40\,^{\circ}\mathrm{C}$ to $120\,^{\circ}\mathrm{C}$ and back to $50^{\circ}\mathrm{C}$ over the course of $3\,\mathrm{h}$. The sample was connected in a 4-wire configuration to a data acquisition unit (34970A, Keysight, USA). Conductive silver glue (SCP, Electrolube, UK) was used to make a connection between the sample and the copper tape traces connected to the data acquisition unit. To get insight in the reputability of this measurement a heating cycle from $30\,^{\circ}\mathrm{C}$ to $70\,^{\circ}\mathrm{C}$ and back over the course of 3 hours was repeated for 4 cycles.

C. Flow sensor characterisation

Figure 3 shows a schematic representation of the measurement setup. The flow was provided by a programmable syringe pump (PHD Ultra, Harvard Apparatus, USA) using syringes with a volume of $15\,\mathrm{mL}$. The flow sensor setup was filled with deionized water, excess of water was collected by a container at the end of the flow sensor.

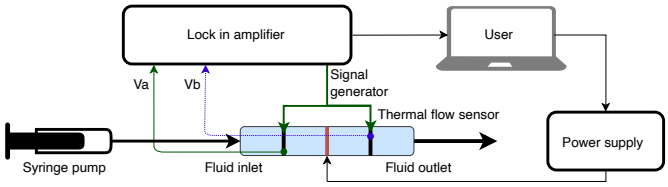

Fig. 3. Measurement setup, V_a and V_b represent the output of upstream and downstream thermal sensors.

The thermal sensors were connected in a voltage divider setup (Figure 4) and read out using a Lock-In Amplifier (SR830 Stanford systems), utilising its signal generator at an amplitude of $1.5\,\mathrm{V}$ and at a frequency of $1.5\,\mathrm{kHz}$. The lock in time constant was set to $10\,\mathrm{ms}$ and the roll off to $12\,\mathrm{dB}$. The output voltage is given by eq. 4 with R_u and R_d being the up- and downstream sensors and R_fixed fixed resistors of the voltage divider.

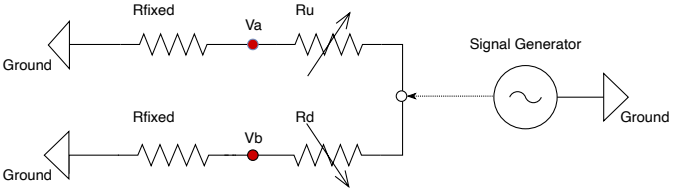

Fig. 4. Voltage divider readout circuit design, R_u and R_d are representing the upstream and downstream thermal sensors.

The output of the sensor can be simulated by modelling the resistance change of the upstream and downstream sensors:

$$R_\mathrm{u} = R_0 + \Delta T_\mathrm{u}\alpha R_0 \qquad R_\mathrm{d} = R_0 + \Delta T_\mathrm{d}\alpha R_0 \tag{3}$$

With ΔT the change in resistance and α the temperature coefficient of resistance (TCR). The resulting expression for V_out is:

$$V_\mathrm{out} = V_\mathrm{b} - V_\mathrm{a} = V_\mathrm{in}\left[\frac{(\Delta T_\mathrm{d} - \Delta T_\mathrm{u})\alpha}{2R_\mathrm{fixed} + (\Delta T_\mathrm{d} + \Delta T_\mathrm{u})\alpha}\right] \tag{4}$$

For the the static characteristics of the heater element, the power was increased gradually in steps of $2\,\mathrm{V}$ ($P = V^2/R_\mathrm{heater}$). The corresponding temperature rise was monitored using a thermocouple placed inside of the channel.

To characterise the output of the sensor with respect to the flow rate, the power of the heater was regulated at $1\,\mathrm{W}$, once the temperature was stabilised, the flow was turned on. The flow was increased in steps of $1\,\mathrm{ml\,min^{-1}}$ to a maximum of $10\,\mathrm{ml\,min^{-1}}$, due to the limited volume of the syringe each flow velocity was measured separately. This measurement is repeated 5 times.

IV. Results

A. Thermal characterisation

Figure 5 shows the change in resistance with respect to temperature. A positive temperature coefficient (PTC) effect

was observed till 110 °C after which the negative temperature coefficient (NTC) effect was seen up till the measurement limit of 120 °C. From Figure 5 (main graph) the non-linear relation of the TCR with respect to temperature can be derived. It displays a superlinear rise from $0.002\,°C^{-1}$ till a maximum of $0.024\,°C^{-1}$ at 110 °C.

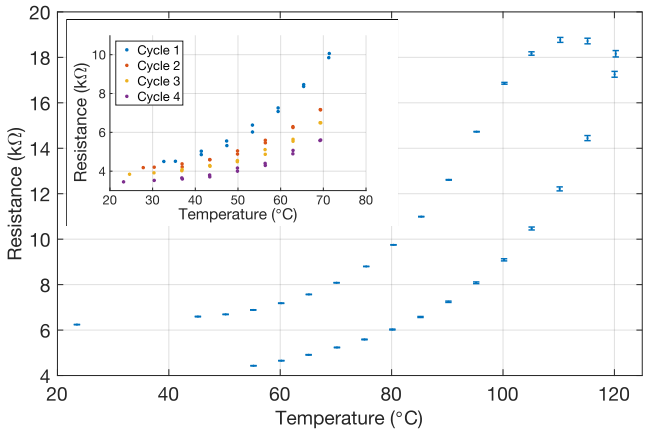

Fig. 5. Resistance over to a 3 hour heating cycle. Insert: Resistance change of four successive heating cycles over 3 hours.

The inset of Figure 5 shows that the resistance dropped after each cycle. However, the influence of temperature on the material is retained and hence can be used for temperature sensitive applications.

B. Flow sensor characterisation

Figure 6 shows the increase of temperature inside of the channel with increasing heater power. Before the start of the flow profile, the temperature increased from 23 °C to a stable 58 °C at a power of 1 W. The measured upstream and downstream resistances were 1.224 kΩ and 1.220 kΩ respectively. The heater resistance was measured 1 kΩ.

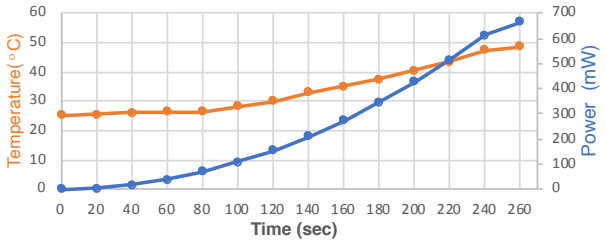

Fig. 6. Temperature in the channel at zero flow with increasing heater power.

Figure 7 shows the modelled and average output of the sensor with respect to the flow rate. For the model a TCR of $\alpha = 0.024\,°C^{-1}$ was taken. This figure shows a linear response of the sensor to flow rates of about $3\,mL\,min^{-1}$ with a sensitivity of $20\,mV/(ml/min)$ with an 1.5 V input voltage. At higher flow velocities the output voltage to flow rate relation flattens and subsequently reverses.

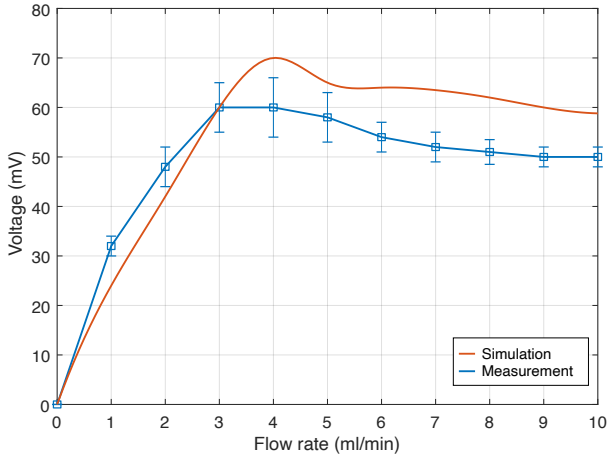

Fig. 7. Model and sensor response to increasing flow rate, measurements are an average over 5 recording, error bars indicate the lowest and highest value.

V. Discussion

Figure 5 shows a positive temperature coefficient (PTC) till 110 °C after which the temperature coefficient becomes negative (NTC). This effect has been reported typically for polymer carbon composites. The PTC effect is thought to be caused by the difference in expansion coefficient between matrix and carbon black filler. Whereas the NTC is assumed to be the result of the formation of conducting networks at higher temperatures, the elastic modulus of the polymer matrix decreases leading to re-connection of the conductive pathways of the filler matrix [13], [14]

The hysteresis shown in Figure 5 might be caused by the thermal capacity of the material causing the cooling of the material to be slower than the environment temperature of the oven. Another explanation could be the annealing effect as show in Figure 5, resulting in a lower resistivity after multiple cycles. A high TCR is desired for sensitive temperature sensing, in comparison the TCR of platinum is $0.0039\,°C^{-1}$ [15], whereas the TCR of PI-eTPU could be as high as $0.024\,°C^{-1}$. In the current design the usable range of the sensor is limited to a flow of $3\,mL\,min^{-1}$. However, by changing the design the sensor can be tuned to a desired range. An application of these flow sensors could be in a 3D-Printed angular acceleration sensor based on the human vestibular system such as demonstrated by van Tiem et. al. [16].

VI. Conclusions

To our knowledge, we have fabricated the first fully 3D-Printed calorimetric flow sensor using FDM technology that uses a conductive filament (PI-eTPU) as both sensing and heater material. The sensor has a close to linear output for flows below $3\,mL\,min^{-1}$ and has a sensitivity of $20\,mV/(ml/min)$. The TCR of PI-eTPU does vary under the influence of temperature but was found to be sufficient to be used for thermal sensing applications.

REFERENCES

[1] K. Adamski, B. Kawa, and R. Walczak, "Inkjet 3d printed venturi microflowmeter," in *2018 XV International Scientific Conference on Optoelectronic and Electronic Sensors (COE)*. IEEE, 2018, pp. 1–3.

[2] L. G. Pagani, P. Carulli, V. Zega, R. Suriano, R. Bernasconi, A. Frangi, M. Levi, L. Magagnin, and G. Langfelder, "The first three-dimensional printed and wet-metallized coriolis mass flowmeter," *IEEE Sensors Letters*, vol. 4, no. 6, pp. 1–4, 2020.

[3] S. Leigh, C. Purssell, D. Billson, and D. Hutchins, "Using a magnetite/thermoplastic composite in 3d printing of direct replacements for commercially available flow sensors," *Smart materials and structures*, vol. 23, no. 9, p. 095039, 2014.

[4] L. Gaffuri Pagani, P. Carulli, V. Zega, R. Suriano, R. Bernasconi, A. Frangi, M. Levi, L. Magagnin, and G. Langfelder, "The first three-dimensional printed and wet-metallized coriolis mass flowmeter," *IEEE Sensors Letters*, vol. 4, no. 6, pp. 6–9, 2020.

[5] M. Schouten, R. Sanders, and G. Krijnen, "3D printed flexible capacitive force sensor with a simple micro-controller based readout," in *2017 IEEE SENSORS*, Oct 2017, pp. 1–3.

[6] S. J. Leigh, R. J. Bradley, C. P. Purssell, D. R. Billson, and D. A. Hutchins, "A simple, low-cost conductive composite material for 3d printing of electronic sensors," *PloS one*, vol. 7, no. 11, p. e49365, 2012.

[7] M. B. Kirkpatrick, J. A. Tarbutton, T. Le, and C. Lee, "Characterization of 3d printed piezoelectric sensors: Determiniation of d 33 piezoelectric coefficient for 3d printed polyvinylidene fluoride sensors," in *SENSORS, 2016 IEEE*. IEEE, 2016, pp. 1–3.

[8] A. Dijkshoorn, P. Werkman, M. Welleweerd, G. Wolterink, B. Eijking, J. Delamare, R. Sanders, and G. J. Krijnen, "Embedded sensing: integrating sensors in 3-d printed structures," *Journal of Sensors and Sensor Systems*, vol. 7, no. 1, p. 169, 2018.

[9] G. Wolterink, R. Sanders, and G. Krijnen, "Thin, flexible, capacitive force sensors based on anisotropy in 3d-printed structures," in *2018 IEEE SENSORS*. IEEE, 2018, pp. 1–4.

[10] ——, "A flexible, three material, 3d-printed, shear force sensor for use on finger tips," in *2019 IEEE SENSORS*. IEEE, 2019, pp. 1–4.

[11] Y.-H. Wang, C.-P. Chen, C.-M. Chang, C.-P. Lin, C.-H. Lin, L.-M. Fu, and C.-Y. Lee, "Mems-based gas flow sensors," *Microfluidics and nanofluidics*, vol. 6, no. 3, p. 333, 2009.

[12] W. Xu, B. Gao, Y.-K. Lee, and Y. Chiu, "Packaging effect on the flow separation of cmos thermoresistive micro calorimetric flow sensors," in *2016 IEEE 11th Annual International Conference on Nano/Micro Engineered and Molecular Systems (NEMS)*. IEEE, 2016, pp. 62–65.

[13] H. Tang, X. Chen, and Y. Luo, "Studies on the ptc/ntc effect of carbon black filled low density polyethylene composites," *European polymer journal*, vol. 33, no. 8, pp. 1383–1386, 1997.

[14] C. Klason and J. Kubat, "Anomalous behavior of electrical conductivity and thermal noise in carbon black-containing polymers at tg and tm," *Journal of Applied Polymer Science*, vol. 19, no. 3, pp. 831–845, 1975.

[15] K. Tsutsumi, A. Yamashita, and H. Ohji, "The experimental study of high tcr pt thin films for thermal sensors," in *SENSORS, 2002 IEEE*, vol. 2. IEEE, 2002, pp. 1002–1005.

[16] J. van Tiem, J. Groenesteijn, R. Sanders, and G. Krijnen, "3d printed bio-inspired angular acceleration sensor," in *2015 IEEE SENSORS*. IEEE, 2015, pp. 1–4.